Instituto de Ciências Matemáticas e de Computação

ISSN - 0103-2577

A Novel Approach for Delaunay 3D Reconstruction with a comparative analysis in the Light of Applications

L.G. Nonato, R. Minghim, M. C. F. Oliveira, G.Tavares.

Nº 55

NOTAS DO ICMC
Série Computação

São Carlos
Dezembro/2000

A Novel Approach for Delaunay 3D Reconstruction with a comparative analysis in the Light of Applications

Luis Gustavo Nonato[1], Rosane Minghim[1], Maria Cristina Ferreira de Oliveira[1], and Geovan Tavares[2]

[1] Departamento de Computação
ICMC/USP - São Carlos
Caixa Postal 668
13560-970 São Carlos - SP
{Nonato, rminghim, cristina}@icmc.sc.usp.br
[2] Pontifícia Universidade Católica do Rio de Janeiro
Departamento de Matemática
PUC - Rio de Janeiro, Brasil
geovan@mat.puc-rio.br

Abstract. This paper presents a novel algorithm for volumetric reconstruction of objects from planar sections using Delaunay Triangulation, which solves the main problems posed to models defined by reconstruction, particularly from the viewpoint of producing meshes that are suitable for interaction and simulation tasks. The requirements for these applications are discussed here and the results of the method are presented. Additionally, it is compared to another commonly used reconstruction algorithm based on Delaunay Trianglulation, showing the advantages of the reconstructions obtained by our technique.

1 Introduction

Computer Visualization technology is gaining wider acceptance in many practical fields, and nowadays it plays an essential role in assisting professionals of different areas. A major visualization problem common to many application fields is the construction of three- dimensional (3D) models from two-dimensional (2D) data. This is a typical problem in Medicine, for example, as two-dimensional (2D) information collected from distinct image acquisition devices may be used to obtain 3D models depicting internal body structures. Resulting models are used in tasks ranging from education and training of students and professionals, to diagnosis, simulation of medical procedures and collaborative surgery.

The work reported in this paper is concerned with the reconstruction problem, which, although having been discussed extensively in the literature, still remains to be completely solved. We present a new algorithm (for the sake or reference, we shall call it Nonato's algorithm), that goes a long way towards reaching that solution. Besides offering an approach to the whole process of reconstructing volumes from planar sections using Delaunay triangulation (DT),

this novel technique, obtained as part of the results in a doctoral thesis [20], offers a theoretical framework for characterizing how DT performs contour connection. We are particularly interested in the quality of the resulting mesh.

The vast majority of reconstruction methods treat only surfaces, which impose difficulties in the case of simulations needed in many applications. Volumetric elements (such as tetrahedrons) are necessary to allow proper interaction tasks, for instance when cutting an object [3]. In that respect, even the methods that reconstruct volume, do not present a good solution for the organization of the resulting volumetric mesh, particularly in the subject of adjacency relationships. We intend to demonstrate that in this paper.

For the goals mentioned above, the solution presented here has managed to meet each one of our requirements, with satisfactory performance, as opposed to any other method we encountered before. Those needs presented themselves when handling a series of visualization applications, and particularly our Virtual Dentistry project, targeted at creating an environment to support education and training of dentistry professionals by means of visualization and simulation of dental procedures. There is undoubtedly great potential for the application of 3D models of teeth and mouth to support activities in Dentistry. Some initial work in this direction is reported in the literature, mainly for mandible reconstruction [24] and chewing simulation [19], as well as some initial reconstruction tasks [10][21]. The dentistry case offers a rich application area to develop, apply and test novel interaction, simulation and visualization tools. In the course of developing such an environment, all the classical and some new difficulties were found concerning the quality of reconstruction.

In the context of the Virtual Dentistry project, we initially analyzed the use of two distinct approaches to create 3D surface models of the internal and external structures of a tooth. One of them used a general- purpose reconstruction package [10] based on Delaunay Triangulation [9] (DT). The other we implemented as an extension to a general visualization library with a reconstruction algorithm applicable to teeth models [25]. This implementation employed a distance-based sampling technique [11] followed by the Marching Cubes algorithm [15]. Such approaches produced good results as far as visual appearance is concerned. However, they presented several of the shortcomings mentioned above, which motivated the exploration of alternative surface and volume reconstruction strategies. Nonato's algorithm, presented here, has performed well in solving these drawbacks. The new method, also based on DT, was compared with both the previous approaches. The results of this comparison are presented.

This paper is organized as follows: section 2 presents a brief description of prior works in three-dimensional reconstruction. In section 3 we review definitions and some properties of the Delaunay triangulation and Voronoi diagram, necessary to the understanding of Nonato's approach. Skeletons and reverse tetrahedrons are also presented in section 3. Section 4 defines contours geometrically well positioned and presents two new propositions about the behavior of the three- dimensional Delaunay triangulation regarding contour connections. Section 5 introduces the treatment of singularities that appear, and the tetra-

hedron subdivision process. Section 6 presents the algorithm itself, and section 7 introduces Geiger's algorithm, used for comparative analysis of our results. Section 8 provides the discussion of these results. Conclusions and further work are discussed in Section 9.

2 Prior Work on 3D Reconstruction

There are three problems that are inherent of the reconstruction process, namely: correspondence, branching and tiling. Correspondence problem arises because only the two-dimensional data are not sufficient to ensure the correct connections of regions in adjacent planar sections. Branching problem is related with saddle points and it appears when the number of regions to be connected is different in each slice. Tiling means to triangulate the strip lying between planar regions to be connected.

There are several strategies to solve the three- dimensional reconstruction problems, such as: implicit, voxel, optimal, deformable and heuristic models. Some of these techniques build the two-dimensional surface that bound the object, and others can generate some representation of the volume within the reconstructed objects.

Implicit surface reconstruction techniques aim at creating a smooth implicit function so that the boundaries of the regions are in the zero set of that function. The work by Jones et al. [11] creates a potential field function based on a signed distance. Then, by interpolating between two consecutive planar sections, the overall implicit function is obtained. With implicit techniques it is possible to ensure that the function created contains the original contours in its zero set. However, guaranteeing that the contours in the surfaces generated are the same as the original ones may be difficult.

Voxel based models visualize the volume of the object directly without building a superficial or volumetric mesh [12]. Though this method can avoid the correspondence, tiling, and branching problems, it is not much appropriated to applications such as numerical simulation. It can, however, be an interesting alternative to visualizing volume information.

Attempts to produce an optimal solution to reconstruction usually employ graph theory. One of the first works in reconstruction from planar sections was developed by Keppel [13]. In this work, the surface bounding the maximal volume of the object under reconstruction is obtained from an optimal search in a graph. Fuchs et al. [8] reconstruct the surface with minimal area making use of a toroidal graph. Shinagawa et al. [26] expand the discrete toroidal graph to form a continuos graph, and homotopy is used for reconstructing parametric surfaces. Meyers et al. [16] assembled contours into cylinders and used a minimum spanning tree to determine the correspondence between them. The optimal approach solves the mesh generation problem but some heuristic is necessary in order to find a solution for the branching problem.

Deformable models use geometry, physics and approximation theory to generate a model of the original object. A good overview of deformable models can

be found in Singh [27]. Objects with complex topology are difficult to handle with this strategy, although Delingette [5] has presented and alternative to this problem.

Heuristic techniques employ some criteria to affect the connections between consecutive regions. The work by Ekoule et al. [6] maps contours into their convex hulls and the shortest edge is used to tile the convex hulls of the contours that are in adjacent levels. The branching problem is solved by creating an intermediate contour between two consecutive slices. Bajaj et al. [2] define three criteria that the reconstructed surface must satisfy and an algorithm is built based in these criteria. In the regions where the conditions cannot be satisfied the surface is completed through a triangulation that takes into account the Voronoi skeleton. Boissonnat [4] uses the three- dimensional Delaunay triangulation for connecting the contours in consecutive slices. His work builds a graph using the projection of the 2D Voronoi Diagrams of every two consecutive slices. From that, a volumetric model is created through tetrahedron elimination. Geiger [9] improves Boissonnat's approach by projecting the two-dimensional Voronoi skeletons from one slice to the adjacent slice in order to handle complicated branching and dissimilar contours. However, in this solution, the problem of treating singularities during the process of tetrahedron elimination remains.

These problem is handled by the new algorithm presented in this paper. It also is based on the Delaunay triangulation, to generate a volumetric model from a sequence of cross sections of an object. We suppose that the input data are non intersecting closed polygonal curves, called contours, that represent the boundary of the regions contained in adjacent slices.

Another important characteristic of our algorithm is that it respects the re-sampling and manifold conditions which can be stated as follows:

1. Re-sampling: The intersections of the model with the original cutting planes give rise to the original regions.
2. Manifold: The model is a three-dimensional piecewise linear manifold.

In section 8 we compare this algorithm with Geiger's algorithm [9], implemented in the Nuages [22] reconstruction software. Both algorithms are capable of reconstructing volumetric objects from contours of interest taken in consecutive parallel cross sections, using tetrahedrons as their volume primitive and the 3D Delaunay triangulation. They can also be used to reconstruct only the surfaces of the 3D objects.

3 Voronoi Diagram and Delaunay Triangulation

A non-void set of points $A = \{x_1, \ldots, x_n\}$ in R^m is in general position if no affine subspace of R^m contains A and there is no sphere S^{m-1} through a subset of A with $m+k$, $k > 1$ points. In this text we will always consider sets of points to be in general position. The Voronoi diagram for A is a decomposition of R^m in convex m-dimensional cells $V_1, ..., V_n$ with the following properties:

1. Each V_i contains one single point x_i of A

2. Given x in R^m, x is in V_i if only if $d(x, x_i) \leq d(x, x_j)$, for every $i \neq j$, where d is the euclidean distance.

From the definition above, it can be shown that the intersection of k, $(2 \leq k \leq m+1)$ Voronoi cells is either empty or a cell with dimension $m-k+1$ contained in the diagram.

The Delaunay triangulation is the geometrical dual of the Voronoi diagram, that is, for each p-dimensional cell of the diagram, we can associate, in a natural way, an $(m-p)$-simplex[1] of the triangulation. For example, in the two-dimensional case, each triangle (2-simplex) is associated to a vertex of the diagram, each edge of the triangulation (a Delaunay edge) is associated to an edge of the diagram, and each vertex x_i is associated to a cell V_i.

It follows, from the duality and from the general position hypotheses, that each 0-dimensional cell of the Voronoi diagram is the center of a sphere circumscribing an m-simplex. An important property that characterizes the Delaunay triangulation in R^m is that the sphere circumscribing a m-simplex does not contain any other point of A in its interior. Moreover, if there exists a sphere passing through $k \leq m+1$ points of A, which does not contain any other point of A in its interior, these k points are the vertices of a $(k-1)$-simplex of the Delaunay triangulation. Good descriptions of the Delaunay triangulation and Voronoi diagram can be found in Fortune [7] and Aurenhammer [1].

When the points of the set A are placed on two consecutive parallel planar sections P_1 and P_2, the intersection of the three-dimensional Delaunay triangulation of the points in A with P_i $(i = 1, 2)$ is identical to the two-dimensional Delaunay triangulation of the points in P_i. This property is presented by Boissonnat [4] and will be useful in our context.

From now on, we suppose that the input set of points is composed by vertices of contours lying on two parallel planar sections.

A problem encountered when using the Delaunay triangulation (DT) to build a model from contours is that some edges of the contours may not belong to the triangulation. Boissonnat [4] has shown that, if we subdivide an edge that does not appear in DT in $O(n)$ new edges, where n is the number of vertices of the contour, we will obtain a new contour (that is contained in the old one), in which all edges are present in the Delaunay triangulation of its vertices. Based on these premises, all contours can be considered to belong to the Delaunay triangulation of their vertices.

3.1 Voronoi Skeletons

Let C_1 and C_2 be two sets of contours contained in adjacent planar sections P_1 and P_2. Let DT be the three- dimensional Delaunay triangulation of the vertices of $C1 \cup C2$. Suppose that the contours in C_1 and C_2 are oriented in such a way that the interiors are always on their right-hand side, and the exterior is on their

[1] A k-simplex is the convex hull of the $k+1$ affinely independent points, i.e., a 3-simplex is a tetrahedron, a 2-simplex is a triangle, and so on.

left- hand side (or vice versa). That way, an edge of DT contained in P_1 or P_2 can be classified as internal or external in accordance to its position inside or outside a region defined by the orientation of the contours. The edges on the contours are labeled as contour edges. Note that only the edges contained in P_i $(i = 1, 2)r$ are classified as internal, external or contour edges. Edges of DT lying between P_1 and P_2 are not classified.

As shown by Boissonnat [4], the intersections of DT with P_1 and P_2 are the two-dimensional Delaunay triangulations of the points in P_1 and P_2. From these intersections and of the duality mentioned above, we can generate the two-dimensional Voronoi diagram in P_1 and P_2.

The internal Voronoi skeleton is defined as the set of edges of the two-dimensional Voronoi diagram contained in P_1 and P_2 which is dual to the internal edges of DT in P_1 and P_2. The external Voronoi skeleton is defined in a similar way in relation to the external edges. These definitions give rise to the definition of internal and external Voronoi skeletons associated to a contour c, which are stated as follows. Let c be a contour in a plane P_i $(i = 1 or 2)$, the internal skeleton associated to c is the subset of edges of the internal Voronoi skeleton contained in P_i that are dual to the internal edges of DT with at least one end in c. The external skeleton associated to c is defined as the subset of edges of the external Voronoi skeleton that are dual to the external edges of DT in P_i with at least one end in c. Figure 1 shows a set of contours and their correspondent internal and external skeletons.

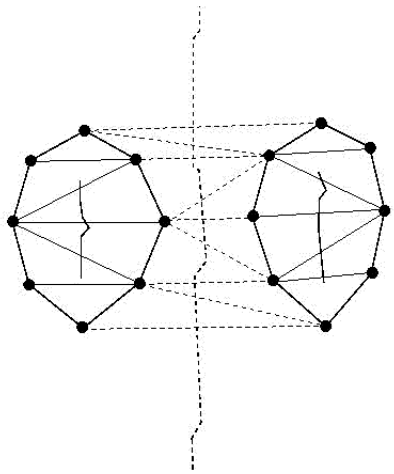

Fig. 1. Internal and external Voronoi skeleton

The skeletons associated to the contours play an important part in the definition of connected components. In the next section we define connected com-

ponents of an object to be reconstructed from the geometrical position of the contours, and we prove that these components can be found by means of topological tests. Before we do that, we need to define an important kind of tetrahedron generated by the three-dimensional Delaunay triangulation, namely the reverse tetrahedron.

3.2 Reverse Tetrahedron

When the set of points A is contained in two consecutive planar sections P_1 and P_2, the three- dimensional Delaunay triangulation generate two kinds of tetrahedrons (see figure 2): tetrahedrons with one face in P_1 (P_2) and one vertex in P_2 (P_1), called tetrahedrons type 1 and tetrahedrons with one edge in P_1 and another in P_2, called tetrahedrons type 2.

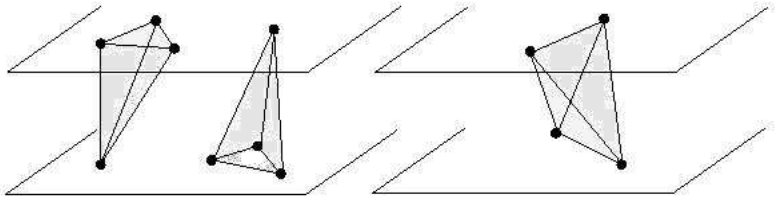

Fig. 2. Tetrahedrons type 1 and type 2

A tetrahedron type 2 is a reverse tetrahedron if both of its edges in P_1 and P_2 are internal edges, or if one of them is internal and the other is an external edge. Figure 3 shows examples of these two cases.

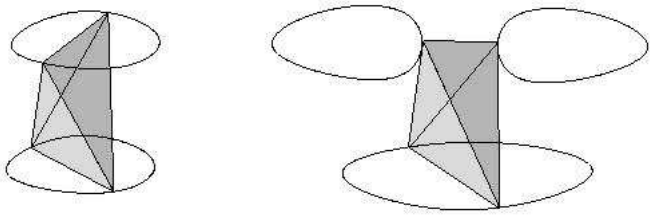

Fig. 3. Reverse tetrahedrons

The reverse tetrahedrons bear a strong relationship with the skeletons associated to the contours. The goal of the next section is to explain what this relationship is.

4 Contours Geometrically Well Positioned

In the field of reconstruction from planar sections, defining which contours should be connected to form a single component is a difficult task, because only the information on contours is not sufficient to guarantee correct correspondence. In this section we present a new heuristic criterion, based on skeletons and on reverse tetrahedrons, in order to define which contours are to be connected. We also prove that this criterion can be obtained by topological tests.

Let C_1 and C_2 be two sets of contours in adjacent planar sections P_1 and P_2.

Definition 1: *Two contours $c_1 \in C_1$ and $c_2 \in C_2$ are geometrically well positioned if the orthogonal projection of the internal skeleton associated to c_1 onto P_2 intersects one of the skeletons (internal or external) associated to c_2, or if the orthogonal projection of the internal skeleton associated to c_2 onto P_1 intersects one of the skeletons associated to c_1.*

It can be noticed, from the definition above, that the contours in adjacent slices with a "strong" overlap are the contours geometrically well positioned. Although definition 1 presents a consistent criterion to verify the position between contours, the computational cost of this verification is high because it demands a large number of intersection calculations. The following proposition supplies a way to obtain the geometrically well positioned contours straightly from the three- dimensional Delaunay triangulation.

Proposition 1: *Two contours $c_1 \in C_1$ and $c_2 \in C_2$ are geometrically well positioned if and only if the three- dimensional Delaunay triangulation of the points in $C_1 \cup C_2$ has a reverse tetrahedron with vertices in c_1 and c_2.*

Proof. Let v_1 and v_2 be edges of the skeletons associated to c_1 and c_2 that intersect each other in the orthogonal projection. Let a be the intersection point. Let d_1 and d_2 be the edges of the Delaunay triangulation in P_1 and P_2 dual to v_1 and v_2. Let S be the sphere through the ends of d_1 and d_2. Note that the center of S belongs to the line defined by the points in v_1 and v_2 that project onto the point a. S does not contain any other point of C_1 or C_2 in its interior. In fact, suppose that there is a point p in P_1 (or P_2) inside S, this point must be inside of the circle generated by the intersection between S and P_1 (P_2). But the center of this circle belongs to v_1 (v_2) and any circle with center in v_1 (v_2) containing the ends of d1 does not have any other point in its interior, then p can not be inside S and (d_1, d_2) defines the reverse tetrahedron in DT.

Let v_1 and v_2 be the edges of the Voronoi diagram dual to the edges d_1 and d_2 of the reverse tetrahedron with vertices in c_1 and c_2. By definition, v_1 and v_2 are edges of the skeletons associated to c_1 and c_2, and the orthogonal projection of v_1 onto P_2 intersects v_2. In fact, let h be the center of the sphere through the vertices of the reverse tetrahedron. The points of the line normal to P_1 and P_2 containing h are equidistant to the ends of d_1 and equidistant to the ends of d_2 so, this line must intersect v_1 and v_2.

A tetrahedron of the three-dimensional Delaunay triangulation is internal to a contour c in P_i if at least one of its edges in P_i is internal to c. A tetrahedron that

has no internal edge and at least one external edge is an external tetrahedron. Note that reverse tetrahedrons are always internal to one or two contours.

Proposition 2: *If two contours $c_1 \in C_1$ and $c_2 \in C_2$ are not geometrically well positioned, then either the internal tetrahedrons of c_1 have no intersection with c_2 or all internal tetrahedrons of c_1 contain a vertex or a contour edge of c_2.*

Proof. If c_1 and c_2 are not geometrically well positioned, proposition 1 ensures that there is not a reverse tetrahedron connecting them. If the internal tetrahedrons of c_1 have no intersections with c_2 the proof is complete. Suppose that the internal tetrahedrons of c_1 have intersections with the contour c_2 and with another contour $\tilde{c}_2 \in C_2$. The intersections with c_2 must be vertices and contour edges of c_2, otherwise c_1 and c_2 would be geometrically well positioned. Let T_1 and T_2 be two internal tetrahedrons of c_1 sharing an internal edge e of c_1 (see figure 4) and suppose that T_1 has vertices in c_2 and that T_2 has vertices in $\tilde{c}_2$. Note that there is a wedge between T_1 and T_2. In order to complete the triangulation it is necessary to have a tetrahedron of type 2 with one edge on e and another edge with ends in c_2 and $\tilde{c}_2$. However, this would be a reverse tetrahedron, so, according to preposition 1, c_2 and c_1 would be geometrically well positioned, which is a contradiction.

The sufficient condition of the proposition is straightforward.

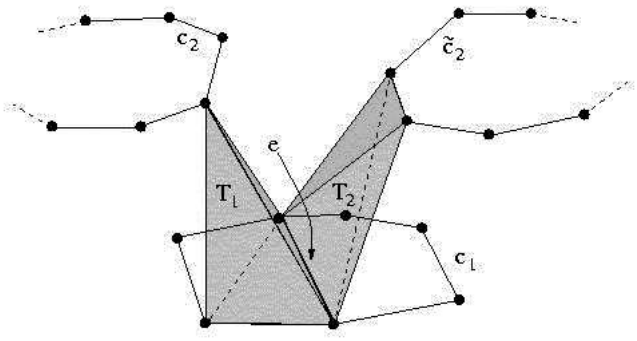

Fig. 4. Contour conections (proposition 2)

The propositions 1 and 2 above completely describe how the three-dimensional Delaunay triangulation connects the contours in adjacent planar sections. An important consequence of these propositions is that, if two contours in adjacent planar sections are not well positioned, an elimination of tetrahedrons along with translations of vertices can be used to separate the components containing these contours, as shown in the figure 5. These premises allow us to define the connected components of the model as follows:

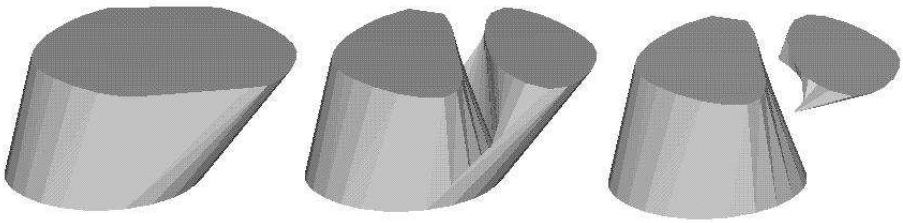

Fig. 5. Delaunay tringularion, tetrahedron elimination and vertices translation

Definition 2: *The connected components of the model are generated by the sets of contours that are geometrically well positioned, i.e., each set of contours geometrically well positioned gives rise to a connected component.*

Definition 2 gives an heuristic to solve the correspondence problem, i.e., to decide which contours are to be connected. In the next section we present a solution to the branching and tiling problems.

5 Singularities

In this section we deal with singularities that appear in the reconstruction process and we show how tetrahedron subdivision can be used in order to eliminate these singularities. Before presenting the singularities we need to understand what they are and how to detect them.

Let DT be the three-dimensional Delaunay triangulation of a set of points. The star of a simplex k in DT is the union of all simplices in DT which contain k. The link of a simplex k is the union of all simplices lying in the star of k that do not contain k. For example, if k is a vertex in DT, the star of k is the union of all tetrahedrons containing k and the link of k is the union of the faces of these tetrahedrons that do not contain k. A vertex is singular if its link is not homeomorphic to a sphere or to a half-sphere and an edge is singular if both its vertices are singular. This definitions provide a tool to find singular vertices and edges. A triangulation is a piecewise linear manifold (PL-manifold) if all its vertices are not singular.

In order to respect the re-sampling condition, i.e., to ensure that the original contours are recovered after intersecting the model with corresponding planes, we must eliminate the external tetrahedrons. However, this elimination can generate singular simplices. For example, the elimination of a reverse tetrahedron with one external edge generates a wedge (a singular edge) in the interior of the contour that contain the internal edge of this reverse tetrahedron. Figure 6 shows this situation.

Our goal is to reconstruct regular objects, i.e., PL-manifold . In order to do so, we must remove the singularities generated by the elimination of the external tetrahedrons. To solve this problem we devised a tetrahedron subdivision process (TSP, for short), which consists of:

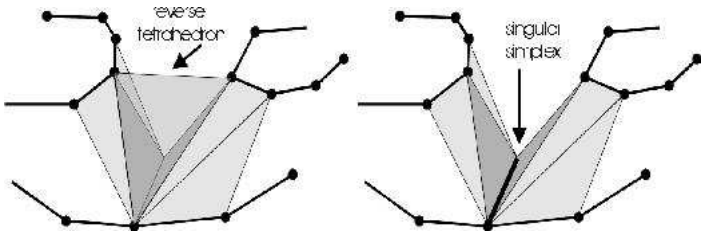

Fig. 6. Singular edge

1. To eliminate the external tetrahedrons which do not generate singularities.
2. To subdivide the external tetrahedrons whose elimination generate singularities.
3. To translate the new points inserted in the subdivision to a position intermediate between consecutive section planes.

The subdivision of tetrahedrons must respect some restrictions:

a) If the tetrahedron is type 1, we insert a new vertex in each external edge. The number of new tetrahedrons depends on the number of new points inserted. For one point, two tetrahedrons; for two points, three tetrahedrons; and for four points, four new tetrahedrons are inserted (see figure 7).
b) If the tetrahedron is type 2, there can be one or two points inserted, according to the external edges. For one new point, two new tetrahedrons are inserted; for two new points, four tetrahedrons, as illustrated in figure 8.

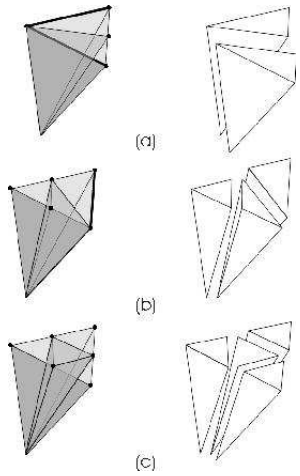

Fig. 7. Subdivision for tetrahedrons type 1

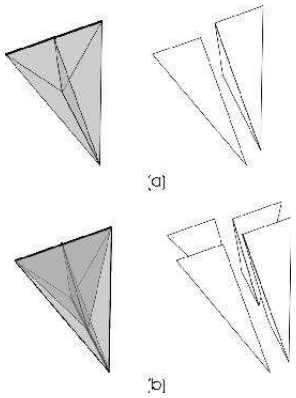

Fig. 8. Subdivision for tetrahedrons type 2

The subdivision of the tetrahedrons respects the contours, i.e., if the tetrahedron to be subdivided has a contour edge, the face containing this contour edge is kept intact. That way, only the faces with external edges are subdivided, all other faces of the tetrahedron are not altered.

The above subdivision process guarantees the manifold condition. In order to ensure the re-sampling condition, we must translate the new points inserted in the subdivision to an intermediate position between the parallel planes. It is important to note that the subdivision of tetrahedrons along with translations of the new vertices solves the branching problem in a very satisfactory way. Figure 9 shows the subdivision and translation processes applied to a reverse tetrahedron, and the solution to branching problem ensuring the re- sampling condition.

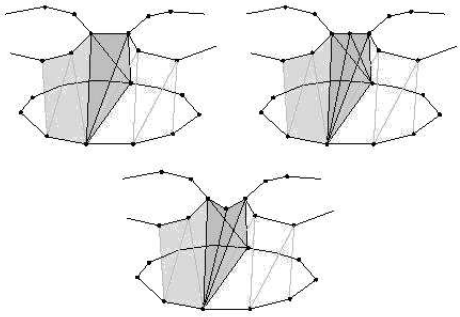

Fig. 9. Subdivision and vertex translation for a reverse tetrahedron

We finish this section with a proposition that is a direct consequence of the discussion above.

Proposition 3: *Let C_1 and C_2 be two sets of contours in adjacent planar sections P_1 and P_2 and DT the three-dimensional Delaunay triangulation of their vertices. The model generated by applying TSP in DT satisfies the re-sampling and manifold conditions to the reconstruction problem.*

6 The Algorithm

In this section we describe the reconstruction algorithm that is derived from the above theory and illustrate its use in some applications such as medicine and terrain reconstruction.

In summary, the algorithm consists in building the three-dimensional Delaunay triangulation, detecting the connected components using reverse tetrahedrons, disconnecting these components according to proposition 2 and applying the tetrahedron subdivision process in each connected component.

In order to separate connected components we must eliminate the external tetrahedrons with vertices in different components and, if necessary, translate vertices, as described in the previous section. Besides the external tetrahedrons, some redundant tetrahedrons must also be eliminated to separate the components. Redundant tetrahedrons are of type 2 with two contour edges. They can appear after the external tetrahedron elimination. Figure 10 shows an example of redundant tetrahedron and its elimination. Proposition 2 guarantees that external and redundant tetrahedron elimination disconnect the components.

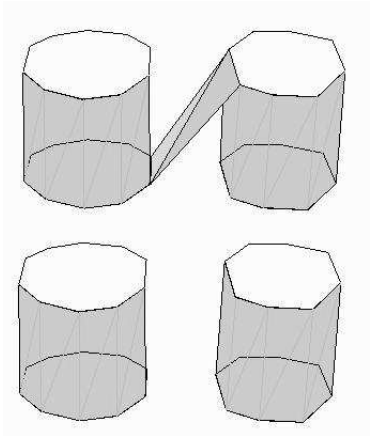

Fig. 10. Redundant tetrahedron elimination

Therefore, Nonato's algorithm can be stated as follows:
Let $C = C1 \cup C2$ be a set of contours in two adjacent planar sections.

1. Compute the 3D Delaunay triangulation of the vertices in C and classify the tetrahedrons as internal, external or reverse.
2. Find the connected components making use of the reverse tetrahedrons.
3. Remove the external and redundant tetrahedrons connecting the components and if necessary translate vertices.
4. For each connected component:
   a) Remove the tetrahedrons whose elimination do not generate singularities.
   b) Remove the redundant tetrahedrons.
   c) Subdivide the external tetrahedrons that can not be eliminated in step (a).
   d) Translate the new vertices to an appropriate position between slices.

The step 1 of the above algorithm generates the three-dimensional Delaunay triangulation and classifies the tetrahedrons. Steps 2 and 3 find and separate connected components of the model. Step 4 is basically the TSP.

It is important to note that geometrical calculations are only necessary to build the Delaunay triangulation. All other operations are topological. This fact ensures a more robust and efficient implementation.

In practical applications, we maintain nested contours in the same connected component, this way decreasing the number of vertex translations and simplifying the implementation.

After the 3D Delaunay triangulation has been built, star and link of simplices are the only necessary operations to be done on the structure. With an appropriate data structure, these topological tests can be executed in linear time [14]. That way, the algorithm complexity is the same as the Delaunay triangulation in R^3, which is $O(n^2)$ by the incremental algorithm [7].

6.1 Examples

Figure 11 shows some examples of objects generated by the algorithm presented here. Figure 11 (a) is a synthetic object with complex geometry and topology, (b) is the Sugar Loaf in Rio de Janeiro reconstructed from level curves, (c) and (d) are models obtained from medical images depicting a vertebra and the lungs. The trachea in figure 11 (d) is disconnected because the original data are too scattered. Note that in map reconstruction, the algorithm always builds a correct model. Since the contours are level curves, the presence of the reverse tetrahedrons is ensured.

6.2 User Intervention

Although our algorithm automatically finds the connected components for the model, it may be adjusted to allow the user to decide how the connections must be made. Contours can be labeled as belonging to the same connected component, prior to reconstruction. In this case, after constructing the Delaunay triangulation for each labeled component, TSP is executed directly, without

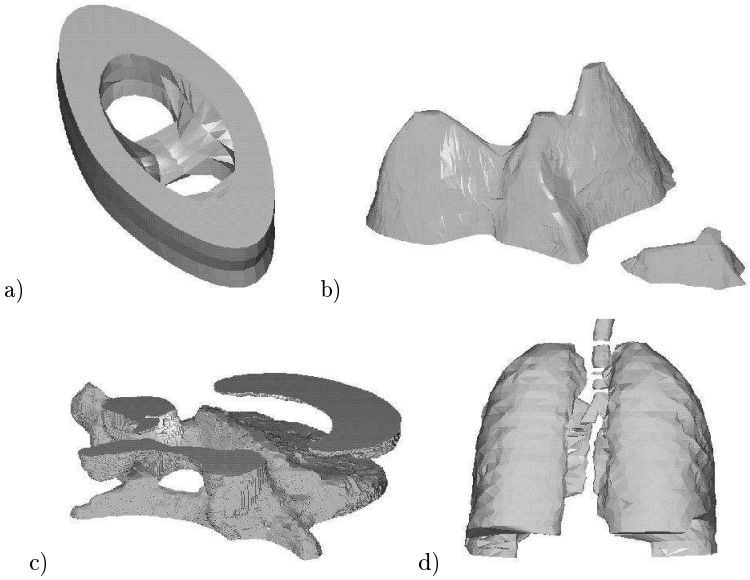

Fig. 11. a) synthetic object b) Sugar Loaf c) vertebra d) lungs

undergoing the step of finding connected components automatically. The results section gives an example of change of connections under user intervention.

This concludes the framework for Nonato's algorithm. It was tested by reconstructing a number of data sets and comparing the results with reconstructions by other methods. Those results are discussed in Section 8. Before that is done, in the next section we describe Geiger's algorithm [9], which is an algorithm of the same class as Nonato's, and that was used for comparison with our results.

7 Geigers Algorithm

Geiger [9] uses the Voronoi skeleton associated with the contours and it consists of three major steps, which are described in the following.

Step 1: 2D triangulation and point inclusions

In this step, the 2D Delaunay triangulation of the contour vertices is calculated and the triangle edges are classified as internal, external or contour edges. If necessary, additional vertices are added on the contour edges to eliminate obtuse triangles. Obtuse triangles elimination is necessary to guarantee that the internal Voronoi skeleton lies inside its contour and that the external Voronoi skeleton lies outside the contours.

The Voronoi skeletons are calculated and the vertices of the external Voronoi skeletons are projected in the adjacent slice. If the projected vertices lie in the interior region of a contour they are added and the triangulation is updated

(figure 12). Projected vertices are included to improve the connection between contours and to avoid jagged shapes.

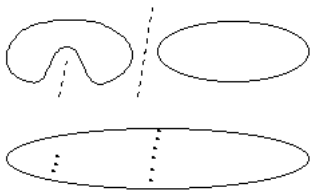

Fig. 12. Voronoi vertices projection

Step 2: 3D Delaunay triangulation

In this step, the 2D Delaunay triangulation is mapped to the 3D Delaunay triangulation. This mapping is based in Boissonnat's algorithm [4], given bellow:

Let A_1 and A_2 be two sets of points on consecutive cross-sections P_1 and P_2. Let D_1, D_2, V_1 and V_2 be the two-dimensional Delaunay triangulation and Voronoi diagrams of the points in A_1 and A_2, respectively (see figure 13 (a)).

The orthogonal projection of V_1 over the plane P_2 joined to V_2 itself, gives rise to a graph G (figure 13 (b)). The nodes of G are either vertices of V_i, $i = 1, 2$ or the result of an intersection of an edge of V_1 with an edge of V_2. All topological and geometrical information of the 3D Delaunay triangulation is contained in G.

If a node v of G is a vertex of V_1 (V_2) then it corresponds to a tetrahedron with one face in P_1 (P_2) and one vertex in $P2$ ($P1$). The face in P_1 (P_2) is the triangle in D_1 (D_2) dual to v, while the vertex in P_2 (P_1) is dual to the Voronoi cell to which the orthogonal projection of v belongs (points 1 and 2 in figure 13(b)).

If v is a vertex in G coming from the intersection of edges in V_1 and V_2 then it corresponds to a tetrahedron built from two edges in D_1 and D_2 dual to these Voronoi edges (points 3 and 4 in figure 13(b)). That way, the 3D Delaunay triangulation is built from the 2D Delaunay triangulation and the Voronoi diagrams of the points in A_1 and A_2, as illustrated in figures 13(c) and (d).

Step 3: Tetrahedral elimination

In order to build a model that approximates the original object, some tetrahedrons have to be eliminated, as it is done in Nonato's algorithm.

In Geiger's algorithm, two kinds of tetrahedrons are eliminated. The first type of tetrahedron are those having an external edge in either P_1 or P_2. The other candidates to elimination are those tetrahedrons whose only connection to either of the two planes lies along an edge or at a single point (figure 14).

One of the basic differences between this strategy and the algorithm presented in section 6 is how they approach the problem of identifying connected

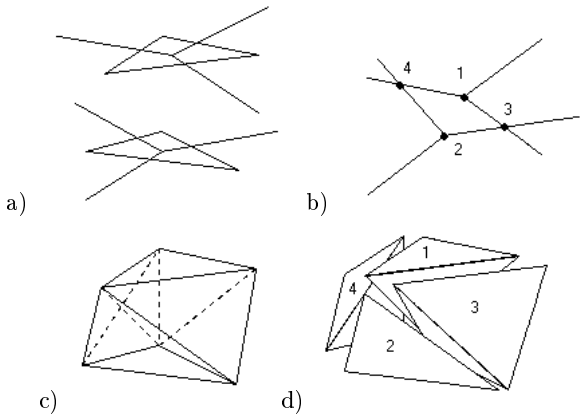

Fig. 13. a) Delaunay and Voronoi 2D b) Graph G c) and d) Delaunay 3D

components. Additionally, elimination of tetrahedrons may introduce singularities that are not eliminated in Geiger's approach, whilst our strategy model such singularities very satisfactorily.

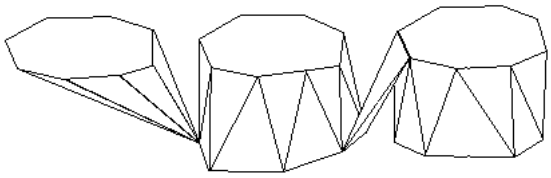

Fig. 14. Singular connections

8 Results

In this section we present some of the results from trying the approaches mentioned in the previous sections to one of our target application (Virtual Dentistry). In the process, some problems concerning data structures, interaction, and visualization of dentistry data are being dealt with by our team and collaborators.

For the tests employing the two reconstruction algorithms discussed here, we concentrated on the present and future needs of such data, and constructed real test cases to check the behavior of both algorithms. The main cases are

presented here, together with the reasons for choosing Nonato's algorithm as the core reconstruction procedure through the next steps in the project.

To test the behavior of Geiger's algorithm, the Nuages public domain reconstruction package was employed [22], and Nonato's algorithm was implemented in the Unix environment.

The results of both, in the form of either a mesh of polygons or a set of tetrahedrons, were stored as VTK data files. VTK (Visualization Toolkit) is an object oriented visualization library with available source code, capable of running and displaying data using most scientific visualization techniques [23]. It runs on Unix and Windows systems, and can be programmed in C++, Java and Tcl/Tk. In the case of this work, it was employed only as a means to visualize our results. Regardless of this, most of our other developments within the Virtual Dentistry project have been implemented as extensions to VTK. As one of our next steps, the chosen reconstruction approach will be adapted to fit into the VTK library.

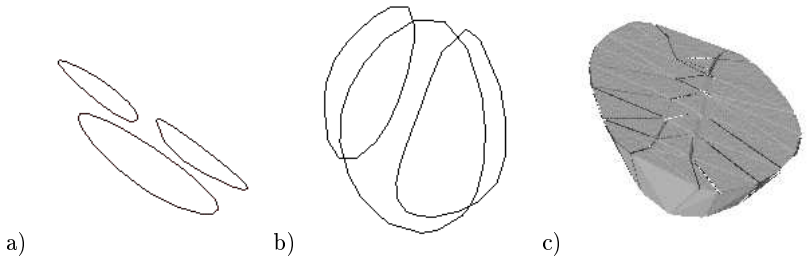

Fig. 15. Bifurcation

We begin this presentation by showing the behavior of both Geiger's algorithm (GA) and Nonato's algorithm (NA) in regards to defining connected components under bifurcation. First, figure 15 shows a bifurcation of contours between neighboring slices, and the result of applying only DT directly to them. As we have seen, both algorithms have different ways of dealing with tetrahedron elimination, which can be seen in figure 16. Figure 16(a) shows a set of contours with a "double-sided" bifurcation. Figure 16(b) shows a view of the reconstruction obtained by GA, while figure 16(c) shows the same set as reconstructed by NA. It can be noted that, when the tetrahedrons are eliminated, GA forms singular edges in the connection. The process of subdivision followed by translation of the mid-point performed by NA avoids these singular edges, whilst maintaining the recovery of contour shape under sampling. Additionally, the GA strategy of tetrahedron elimination causes the connection between the two sides of the structure to be blocked (see figure 16(d)), while the strategy in NA generates a tunnel between them (figure 16(e)). For dental and some other organic structures, this topology seems to fit better than the former, blocked,

structure. Besides, the singular edge makes it difficult to determine behavior of an object subjected to numerical simulations, which is one of our intents during interaction with the models. Figures 16(f) and (g) show detail of the two different triangulations in the connection where tetrahedrons were deleted.

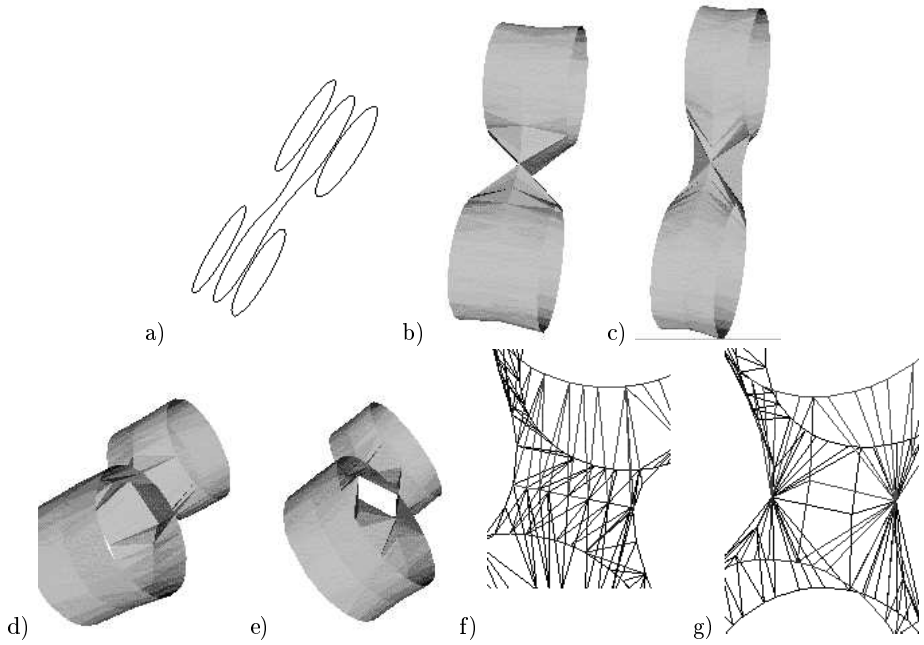

Fig. 16. Handling of bifurcation and tetrahedron elimination.

The next step of the tests was meant to verify how the definition of connected components behaved, particularly over bifurcation. To do that, we first tested the reconstruction for the contours presented in figure 15(a) and 15(b) by both GA and NA. The result can be observed in figures 17(a) and 17(b), which show the reconstructions from the bottom, without closing the model, so as to observe the connections made. For GA, we can observe that a sequence of edges is created that lies in the region enclosed by the bottom slice. Consequently, if the model were cut by the same plane that originally generated the slices, the contours obtained would be different from the original ones. In fact, the bottom slice shows the contour divided in two, while, originally, it was a single contour. The strategy of NA causes the model to be consistent with the original slice set, if sampled in the same way.

Following this test, we drifted one of the contours of the set (the top left contour) aside, so that overlapping between orthogonal projections of the two slices was decreased. In the case of GA (figure 18(a)), all the edges on one

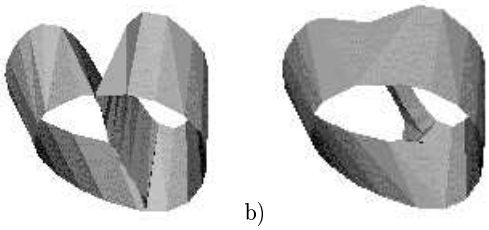

a) b)

Fig. 17. Handling of bifurcation.

contour fell on the edge of the bottom contour. NA, however, can behave in two different ways. Left to itself, components are connected as shown in figure 18(b), that is, the components are actually disconnected, and both contours preserved. Under user choice, these components can be connected, in a similar fashion as the previous model, forming a single object that also preserves the integrity of the original contour set (figure 19). Here, too, we find that keeping the original contours is an important aspect for our application, which causes us to lean again towards NA.

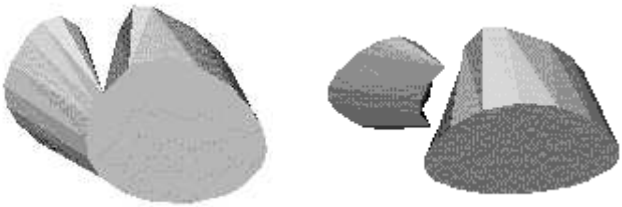

a) b)

Fig. 18. Handling of connected components when the contous are apart

To illustrate what happens when one contour really drifts apart, making no overlapping with any of the consecutive slices, we refer to figure 20. In this case, using the set of contours in figure 20(a), GA chooses not to reconstruct the 'extra' contour (figures 20(b) and 20(c)). That happens because, during reconstruction, all the connections between the isolated contour and the rest of the model occur on a single vertex. Although this is a very particular case, it is a perfectly plausible situation when reconstructing some small body structures.

For the same set, NA, performs the referred reconstruction and initially defines it as a separate component (figures 20(d) and 20(e)) (as in the other cases, it uses the reverse tetrahedron criterion).

Fig. 19. User intervention (alternative to figure 18 (b))

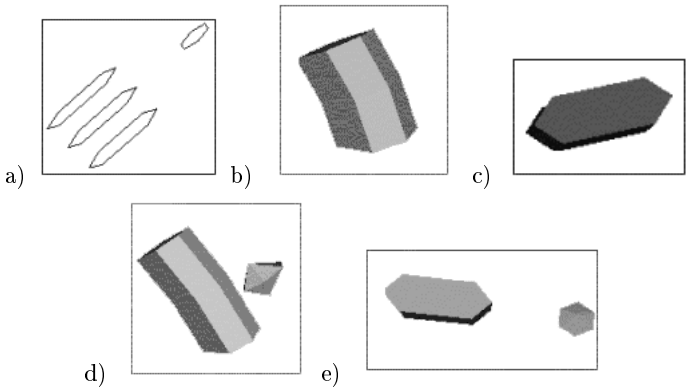

Fig. 20. Handling of isolated contours

The last test we report here was performed to observe the results of the reconstruction of both approaches in the case of the tooth data. For that, we had a set of tooth contours edited from real data[10], containing one internal and one external surface (figure 21(a)). NA built the whole set with no detectable errors or inconsistencies (see figure 21(b)), both for separate sets (internal and external) and for nested contours. In this reconstruction case, there were difficulties running the package for GA, due to execution errors. In short, there were quite a few slices in the set that simply could not be processed, as shown in figure 21(c). This is possibly due to the fact that the projection realized by the method is subject to numerical instability. In some cases, perturbation forced on the original point set helped the missing slices to be reconstructed. Additionally, a few 'spurious' triangles showed up in the reconstruction unexpectedly, as illustrated by figure 22.

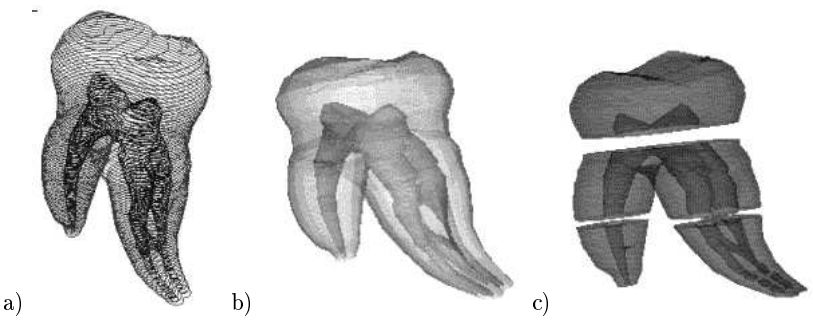

Fig. 21. Tooth case

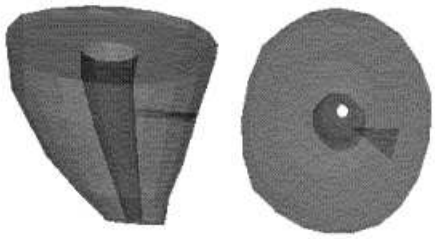

Fig. 22. Inconsistency in triangulation as built using NUAGES

Numerical instability for NA is kept under control mainly because the only time when geometrical operations are performed is during the calculation of

the 3D Delaunay Triangulation. All other tests (including proximity tests) are performed topologically.

Both GA and NA reconstruct the volume, that is, the interior of the object is filled with tetrahedrons. That is also a requirement for the Virtual Dentistry Project, if we are to simulate realistic situations during interaction.

The tests mentioned above confirmed our expectation of the types of improvement that Nonato's algorithm can bring over previous reconstruction algorithms based on Delaunay Triangulation, leading to the choice of using it as the basis for our reconstruction tasks.

Next section presents some of our conclusions from this work.

9 Conclusions and further work

In this paper we presented a novel technique for approaching volumetric reconstruction of 3D structures from planar contours. This technique solves the main problems encountered in building a robust 3D model of those structures, as well as offering a theoretical foundation for the nature of connections generated by 3D Delaunay triangulation. To validate the implementation we compare the results of this technique with another method for the same type of volumetric reconstruction. We demonstrate the advantages of Nonato's algorithm over this previous approaches. Another work that we have carried on previously also offered a general comparison between DT based reconstruction techniques and methods based on volume sampling, providing a list of requirements met by DT that are not handled well by sampling (and fitting) methods [21]. That completes the validation of Nonato's method, put forward for the first time in this paper.

We used as base for our discussions several situations that occurred when we were dealing with data in some application, particularly the Dentistry domain. The tests conducted indicated that Nonato's algorithm presents good behavior in critical situations, typical of reconstruction tasks in several applications. The algorithm produces robust models suitable for undergoing numerical procedures required by simulation processes. This is a major requirement to be met in the Virtual Dentistry project as well as other visualizations we are working on. The method does that by, opposed to other known techniques for volumetric reconstruction, solving well the problem of producing meshes with no singularities. This frees calculations during simulation of physical phenomena from the costly task of having to detect and 'go round' singular edges and vertices. As a result of the comparisons realized between this and other known reconstruction methods, Nonato's algorithm has been chosen as the reconstruction basis in our target systems.

The method itself is currently being re-coded for use as an extension to VTK. This should allow a larger number of researchers and users to test its features in their own application in the near future.

The next topic for investigation will be the simulation of dental procedures over the volumetric models produced. We are also investigating the use of Direct Volume Rendering Methods [12] for visualizing Dentistry data as an alternative

to geometric based models [28] and the integration of both approaches17. DVR techniques present some advantages over the Delaunay based approaches discussed here. One of them is that it preserves more information from the data set, which can, for example, allow easier observation of tissue. Another significant advantage is that it does not require a previous segmentation step, which may be critical. Achieving real time user interaction, however, may pose a major problem, as most DVR algorithms are computationally expensive.

Real Time interaction over the reconstructed volumes, using Virtual Reality, is also a subject of our interest, to be handled in order to provide a full system for training in dentistry and other areas, such medicine and object analysis for agricultural purposes. One particular problem, not addressed by fitting strategies, and overcome by Nonato's method is the possibility of defining a data structure that is effective for real time user interaction and manipulation. This is an essential requirement, as one of our goals is to provide an exploratory environment. Also, to support simulation of dental procedures it is convenient to have volumetric models suitable for manipulation by numerical analysis procedures, such as finite element methods. The data structure, under development, must be capable of indexing each element in a way that is appropriate for both intents: interaction and simulation, as their functions will have to be provided simultaneously. Additionally, we are studying ways of blending the information generated by DVR into the indexing methodology of the data structures, as a way to provide an integrated environment, capable of handling directly and indirectly rendered pictures simultaneously.

Most of our developments are progressively becoming available on the internet, as will most of the dentistry visualization system [18].

The simulation tasks are being developed in collaboration with the numerical simulation group at our lab LCAD (http://www.lcad.icmc.sc.usp.br), whose vast experience in computational fluid dynamics will be of advantage for the dentistry case.

Acknowledgements

We wish to acknowledge the following people for the data employed in the visualizations: M. Goetz and A. Day (UEA - UK) for the tooth data; G. Barequet (Tel Aviv University) for the spine data; B. Geiger (INRIA- France) for the lung data; and M. Grivet (PUC-Rio) for the Sugar Loaf data.

Acknowledgments are also due to FAPESP and CNPq, two Brazilian financial agencies, whose funds made this work possible.

References

1. F. Aurenhammer, Voronoi Diagrams A Survey of a Fundamental Geometric Data Structure. ACM Computing Surveys, 23(3), pp. 345-405, 1991.
2. C.L. Bajaj, E.J. Coyle and K. Lin, Arbitrary topology shape reconstruction from planar cross sections. Graphical Models and Image Processing, 58(6), pp. 524543, 1996.
3. D. Bielser and M. H. Gross, Interactive Simulation of Surgical Cuts. IEEE Computer Society Press (Proceedings of Pacific Graphics'2000), pp. 116- 125, 2000.

4. J-D. Boissonnat, Shape Reconstruction from Planar Cross Sections. Computer Vision, Graphics and Image Processing, (44), pp. 1-29 1988.
5. H. Delingette H., Simplex Meshes: A General Representation for 3D Shape Reconstruction. Technical Report 2214, INRIA, 1994.
6. A. B. Ekoule, F. C. Peyrin, C. L. Odet, - A Triangulation Algorithm from Arbitrary Shaped Multiple Planar Contours. ACM Trans. on Graph., 10(2), pp. 182-199, 1991.
7. S. Fortune, Voronoi Diagrams and Delaunay Triangulation. Computing in Euclidean Geometry (D-Z. Du, F K. Hwang eds.), Wor1d Scientific Pub. Co., pp. 193-233 1994.
8. H. Fuchs, Z.M. Kedem, S.P. Uselton, Optimal Surface Reconstruction from Planar Contours. Communications of the ACM, 20(10), pp. 693-702, 1977.
9. B. Geiger, Three Dimensional Modeling of Human Organs and its Application to Diagnosis and Surgical Planning. Technical Report 2105, INRIA (Sophia-Antipolis), France 1993.
10. M.R. Goetz, A.M. Day, Surface Reconstruction for Teeth. Proc. EUROGRAPHICS98, 16th Annual Conference, March, Leeds, UK, pp. 25-27, 1998.
11. M.W. Jones, M. Chen, A New Approach to the Construction of Surfaces from Contour Data. Proc. EUROGRAPHICS94, 13(3), pp. 75-84, 1994.
12. A. Kaufman, Advances in Volume Visualization. SIGGRAPH98 (Course Notes no. 24), Orlando, 1998.
13. E. Keppel, Approximating complex surface by triangulation of contour lines. IBM. J. Res. Dev. 19, pp. 2-11, 1975.
14. H. Lopes, L.G. Nonato, S. Pesco, G. Tavares, Dealing with Topological Singularities on Volumetric Reconstruction. Curves and Surfaces Design (J-P. Laurent, P. Sablonniere, L.L. Schumaker eds.), Vanderbilt University Press, pp. 229-238, 1999.
15. W. E. Lorensen, H. E. Cline, Marching Cubes: A High Resolution 3D Surface Construction Algorithms. ACM SIG. Comp. Graph. (21), 163- 169, 1987.
16. D. Meyers, S. Skinner, K. Sloan, Surface from Contours. ACM Trans. on Graphics, 11(3), pp. 228258, 1992.
17. R. Minghim, I. P. Soares, M. C. F. Oliveira, L. G. Nonato. Combination of Techniques to Enrich Visualization in Dentistry. ICMC-USP Technical Report, 2000.
18. A. D. Alves, M. C. F. de Oliveira, R. Minghim, L. G. Nonato. Interactive Visualization over the WWW. IEEE Computer Society (Proceedings of SIBGRAPI 2000), pp. 259-266, 2000.
19. K. Myszkowski, G. Okuneva, J. Herder, T. L. Kunii, T.L, M. Ibusuki, Visual Simulation of the Chewing Process for Dentistry. Visualization and Modelling, Academic Press, pp. 419-438, 1997.
20. L.G. Nonato, Volumetric Manifold Reconstruction from Planar Sections. Ph.D. Thesis (in Portuguese), Mathematics Dep., Pontifical Catholic University, Rio de Janeiro, Brazil, 1998.
21. L.G. Nonato, R. Minghim, M.H. Shimabukuro, Qualitative Analysis of Reconstruction Techniques for Dentistry. accepted for publication in the J. of Electronic Imaging, 2000.
22. [NUAGES] http://www.inria.fr/prisme/personnel/geiger/nuages. html, visited in September 2000
23. W.J. Schröeder, K. Martin, W. Lorensen, The Visualization Toolkit, An Object-Oriented Approach to 3D Graphics 2nd. ed., Prentice-Hall, 1998.
24. S. Seipel, I. Wagner, S. Koch, W. Scheneider, Three-dimensional Visualization of the Mandible: A New Method for Presenting the Periodontal Status and Diseases. Comput. Meth. Programs Biomed. (46), pp. 51-57, 1995.

25. M.H. Shimabukuro, R. Minghim; P. Licciardi, Visualization and Reconstruction in Dentistry. IEEE CS Press (Proc. Int. Conf. on Information Visualisation IV98, London, UK), pp. 25-31, 1998.
26. Y. Shinagawa, T.L. Kunii, The homotopy model: a generalized model for smooth surface generation from cross sectional data. The Visual Computer, (7) pp. 7286, 1991.
27. A. Singh, D. Goldgof, D. Terzopoulos (ed.), Deformable Models in Medical Image Analysis. IEEE CS Press, 1998.
28. I. P. Soares, I. P., R. Minghim, M. C. F. Oliveira, L. G. Nonato, Implementing and Applying Direct Volume Rendering with Textures. ICMC-USP Technical Report, 2000